Inorganica Chimica Acta 363 (2010) 2080–2088

Contents lists available at ScienceDirect

Inorganica Chimica Acta

journal homepage: www.elsevier.com/locate/ica

Arylazoimidazoliumchloride and chlorometallates: Spectroscopic and structural characterization

S. Halder [a], G. Saha [a], B.G. Chand [a], A.D. Jana [b], G. Mostafa [b], J. Cheng [c], T.-H. Lu [c], C. Sinha [a,*]

[a] Department of Chemistry, Inorganic Chemistry Section, Jadavpur University, Kolkata, West Bengal 700032, India
[b] Department of Physics, Jadavpur University, Kolkata, West Bengal 700032, India
[c] Department of Physics, National Tsing Hua University, Hsinchu 300, Taiwan, ROC

ARTICLE INFO

Article history:
Received 29 May 2009
Received in revised form 2 February 2010
Accepted 5 February 2010
Available online 12 February 2010

Keywords:
Aryl-azo-imidazolium chloride
Chlorometallated azoimidazolium
X-ray structures
Tapelike aquated-chloride
Ladder

ABSTRACT

Protonation or dialkylation of 2-(arylazo)imidazoles (RaaiH) has generated azoimidazolium motif (RaaiH$_2^+$, RaaiR$'$H$^+$, RaaiR$'_2{}^+$ where R = H, CH$_3$ and R$'$ = Me, Et, –CH$_2$Ph). Electrostatic attraction between imdazolium cation and counter ions like Cl$^-$, ZnCl$_4^{2-}$, PtCl$_6^{2-}$ has generated hydrogen bonded azoimidazolium-chloride/chlorometallated networks. The single crystal X-ray structure of 1-benzyl-2-(phenylazo)imidazolium chloride shows tape like 1-D network of [Cl(H$_2$O)$_4$]$^-$. Aquated Cl$^-$ forms 10 membered supracycle through hydrogen bonding with imidazolium ion. The X-ray structures of [HaaiMe$_2$ (1,3)]$^+$[Me$_2$NH$_2$]$^+$ [ZnCl$_4$]$^{2-}$ and [MeaaiH$_2^+$·H$_2$O]$_2$[PtCl$_6$]$^{2-}$ show hydrogen bonded chlorometallate chain penetrated into the channel developed by organic motif. Azoimidazolium units are associated through π···π and C–H···π interactions to strengthen the supramolecular geometry.

1. Introduction

Anion receptors are of considerable current interest in molecular recognition study [1–4]. Electrostatic interaction, hydrogen bonding, D–H···A (D = donor, A = acceptor), D–H···π, and π···π interactions have been exploited to recognize the anions. Protonated amines or quaternary ammonium ions present in a ligand topology make attractive receptors for anions [1,4–9]. Azole based H-receptors (containing N–H unit as hydrogen donor) are effective binding agents [10–12]. Presence of electron withdrawing substituents on the aromatic part has significantly improved the stability of anion binding [13]. We are engaged for last several years in the design of azo functionalized imidazole molecules [14,15] and have been used to study the anion binding property [16,17]. Halides (X$^-$), bihalides (HX$_2^-$), pseudohalides have been encapsulated in different cavities in view of their participation in important chemical and biological processes [3,4,18]. In this work we have used azoimidazolium ion to bind Cl$^-$ and chlorometallates, like tetrahedral [ZnCl$_4$]$^{2-}$ and octahedral [PtCl$_6$]$^{2-}$ to prepare ionic solids. Crystal structures of the compounds reveal that the hydrogen bonds, C–H···π and π···π interaction present to constitute supramolecular geometry.

2. Experimental

2.1. Materials

ZnCl$_2$, H$_2$PtCl$_6$ were purchased from Aldrich–Sigma. 1-alkyl-2-(arylazo)imidazoles were synthesized by reported procedure [14]. All other chemicals and solvents were reagent grade as received.

2.2. Physical measurements

Microanalytical data (C, H, N) were collected on Perkin–Elmer 2400 CHNS/O elemental analyzer. Spectroscopic data were obtained using the following instruments: UV–Vis spectra from Perkin–Elmer Lambda 25 spectrophotometer; IR spectra (KBr disk, 4000–450 cm^{-1}) from Perkin–Elmer RX-1 FTIR spectrophotometer and ^{1}H NMR spectra from Bruker (AC) 300 MHz FTNMR spectrometer. Molar conductance was measured using Systronics-304 conductivity meter.

2.3. Preparation of compounds

2.3.1. Preparation of 1-methyl-2-(phenylazo)imidazolium chloride (HaaiMeH$^+$Cl$^-$)(**2a**)

To methanolic solution (10 ml) of 1-methyl-2-(phenylazo)imidazole (0.2 g, 1.08 mmol), HCl solution (6 N) (1 ml) was added and left for several days to evaporate. Orange crystalline compound

---

* Corresponding author. Tel.: +91 033 2414 6666x2458(O); fax: +91 033 2414 6584.

E-mail address: c_r_sinha@yahoo.com (C. Sinha).

0020-1693/$ - see front matter © 2010 Elsevier B.V. All rights reserved.
doi:10.1016/j.ica.2010.02.006

was separated, then filtered and washed with cold water. Residue was redissolved in minimum volume of warm water and slowly evaporated. Orange needle shaped crystals were isolated by filtration. Yield: 0.16 g (67%). The reactions are summarized in Scheme 1.

All other compounds were prepared by identical procedure in the yield of 65–80%. Microanalytical data are: $[HaaiH_2^+]Cl^-$ (**1a**), *Anal.* Calc. for $C_9H_9N_4Cl$: C, 51.80; H, 4.32; N, 26.86. Found: C, 51.68; H, 4.27; N, 26.58%; UV–Vis (methanol), $\lambda_{max}(\varepsilon \times 10^{-4}, mol^{-1}\,cm^{-1})$: 380 (2.13), 273 (8.15). $[MeaaiH_2^+]Cl^-$ (**1b**), *Anal.*Calc. for $C_{10}H_{11}N_4Cl$: C, 53.93; H, 4.94; N, 25.17. Found: C, 53.80; H, 4.88; N, 25.24%; UV–Vis (methanol), $\lambda_{max}(\varepsilon \times 10^{-4}, mol^{-1}\,cm^{-1})$: 376 (3.45), 280 (9.05). $[HaaiMeH^+]Cl^-$ (**2a**), *Anal.*Calc. for $C_{10}H_{11}N_4Cl$: C, 53.93; H, 4.94; N, 25.17. Found: C, 53.85; H, 4.91 N, 25.28%; UV–Vis (methanol), $\lambda_{max}(\varepsilon \times 10^{-4}, mol^{-1}\,cm^{-1})$: 382 (3.10), 270(7.89). $[MeaaiMeH^+]Cl^-$ (**2b**), *Anal.* Calc. for $C_{11}H_{13}N_4Cl$: C, 55.81; H, 5.50; N, 23.68. Found: C, 55.85; H, 5.44; N, 23.61%; UV–Vis (methanol), $\lambda_{max}(\varepsilon \times 10^{-4}, mol^{-1}\,cm^{-1})$: 380 (2.30), 270 (8.00). $[HaaiEtH^+]Cl^-$ (**3a**), *Anal.* Calc. for $C_{11}H_{13}N_4Cl$: C, 55.81; H, 5.50; N, 23.68. Found: C, 55.74; H, 5.45; N, 23.60%; UV–Vis (methanol), $\lambda_{max}(\varepsilon \times 10^{-4}, mol^{-1}\,cm^{-1})$: 381 (3.54), 270 (7.54).. $[MeaaiEtH^+]Cl^-$ (**3b**), *Anal.* Calc for $C_{12}H_{15}N_4Cl$: C, 57.49; H, 5.99; N, 22.36. Found: C, 57.55; H, 6.06; N, 22.26%; UV–Vis (methanol), $\lambda_{max}(\varepsilon \times 10^{-4}, mol^{-1}\,cm^{-1})$: 383 (1.88); 277 (7.78).. $[Haai(CH_2Ph)H^+]Cl^-$ (**4a**), *Anal.* Calc. for $C_{16}H_{15}N_4Cl$: C, 64.32; H, 5.03; N, 18.76. Found: C, 64.25; H, 5.00; N, 18.68%; UV–Vis (methanol), $\lambda_{max}(\varepsilon \times 10^{-4}, mol^{-1}\,cm^{-1})$: 390 (5.89), 283(8.55). $[Meaai(CH_2Ph)H^+]Cl^-$ (**4b**), *Anal.* Calc. for $C_{17}H_{17}N_4Cl$: C, 65.28; H, 5.44; N, 17.92. Found: C, 65.34; H, 5.50; N, 18.00%; UV–Vis (methanol), $\lambda_{max}(\varepsilon \times 10^{-4}, mol^{-1}\,cm^{-1})$: 386 (4.54), 278 (8.45).

2.3.2. Preparation of 1,3-dimethyl-2-(phenylazo)imidazolium chloride $[HaaiMe_2^+]$ (Cl^-)(*5a*)

To dry THF solution (20 ml) of 2-(phenylazo)imidazole (HaaiH) (0.2 g, 1.16 mmol), NaH (50% paraffin) was added in pinch and stirred for 30 min. Methylchloride (0.15 g, 3.0 mmol) was added in dropwise for 10 min. and refluxed for additional 2 h then cooled and filtered. Filtrate was evaporated in vacuum. Dry residue was extracted with $CHCl_3$ and was filtered. The orange residue was dissolved in minimum volume warm water and filtered. Filtrate was evaporated slowly and crystalline products were collected. Yield. 0.21 g (76%).

All other compounds were prepared by identical procedure in the yield of 70-80%.

Microanalytical data are: $[HaaiMe_2^+]Cl^-$ (**5a**), *Anal.* Calc. for $C_{11}H_{13}N_4Cl$: C, 55.81; H, 5.50; N, 23.68. Found: C, 55.72; H, 5.42; N, 23.58%; UV–Vis (methanol), $\lambda_{max}(\varepsilon \times 10^{-4}, mol^{-1}\,cm^{-1})$: 375(4.40), 275(6.15). $[MeaaiMe_2^+]Cl^-$ (**5b**), *Anal.* Calc. for $C_{12}H_{15}N_4Cl$: C, 57.49; H, 5.99; N, 22.36%. Found: C, 57.55; H, 6.05; N, 22.24%; UV–Vis (methanol), $\lambda_{max}(\varepsilon\, x\, 10^{-4}, mol^{-1}\,cm^{-1})$: 383 (2.30), 270(8.23). $[HaaiEt_2^+]Cl^-$ (**6a**), *Anal.* Calc. for $C_{13}H_{17}N_4Cl$: C, 58.98; H, 6.43; N, 21.17. Found: C, 59.06; H, 6.48; N, 21.25%. $[MeaaiEt_2^+]Cl^-$ (**6b**), *Anal.* Calc. for $C_{14}H_{19}N_4Cl$: C, 60.32; H, 6.82; N, 20.11. Found: C, 60.40; H, 6.85; N, 20.24%; UV–Vis (methanol), $\lambda_{max}(\varepsilon \times 10^{-4}, mol^{-1}\,cm^{-1})$: 382 (3.10), 270 (7.10). $[Haai(CH_2Ph)_2^+]Cl^-$ (**7a**), *Anal.* Calc. for $C_{23}H_{21}N_4Cl$: C, 71.04; H, 5.41; N, 14.41. Found: C, 71.10; H, 5.50; N, 14.35%; UV–Vis (methanol), $\lambda_{max}(\varepsilon \times 10^{-4}, mol^{-1}\,cm^{-1})$: 385 (4.25), 280 (8.140. $Meaai(CH_2Ph)_2^+]Cl^-$ (**7b**), *Anal.* Calc. for $C_{24}H_{23}N_4Cl$: C, 71.55; H, 5.71; N, 13.91. Found: C, 71.60; H, 5.75; N, 14.00%; UV–Vis (methanol), $\lambda_{max}(\varepsilon \times 10^{-4}, mol^{-1}\,cm^{-1})$: 390 (3.55), 280 (7.86).

.

2.4. Preparation of azoimidazolium chlorometallates

2.4.1. $[HaaiH_2^+]_2ZnCl_4^{2-}$ (*8a*)

An aqueous solution of $ZnCl_2$ (30 mg, 0.122 mmol) in dilute HCl (1:1, v/v) (5 ml) was added in dropwise to methanolic solution (10 ml) of HaaiH (40 mg, 0.23 mmol). Orange solution was allowed to evaporate slowly for a week at 15 °C. Crystals were deposited on

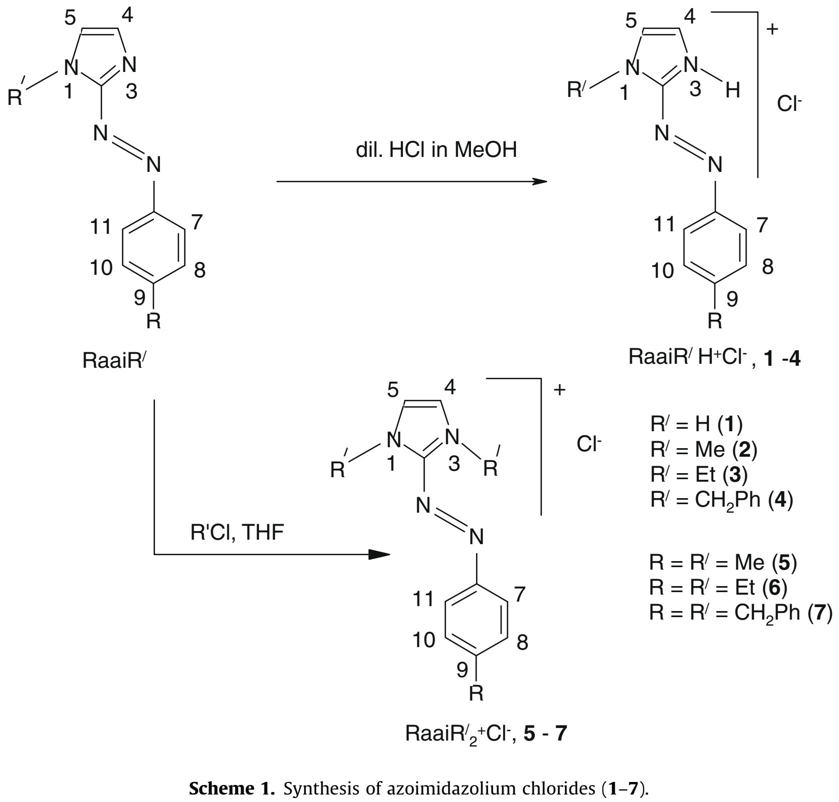

Scheme 1. Synthesis of azoimidazolium chlorides (**1–7**).

the wall of beakers and collected by filtration and dried over $CaCl_2$ in desiccator. Yield: 37 mg (54%).

All other compounds were prepared by identical procedure in the yield of 50–70%.

All other compounds were prepared by identical procedure in the yield of 50–70%. Microanalytical data are: $[HaaiH_2^{+}]_2ZnCl_4^{2-}$ (**8a**): *Anal.* Calc. for $C_{18}H_{18}N_8Cl_4Zn$: C, 39.04; H, 3.25; N, 20.24. Found: C, 39.11; H, 3.27; N, 20.17%; UV–Vis (methanol), $\lambda_{max}(\varepsilon \times 10^{-4}$, mol^{-1} cm^{-1}): 388 (2.08), 285(7.88). $[MeaaiH_2^{+}]_2[ZnCl_4^{2-}]$ (**8b**): *Anal.* Calc. for $C_{20}H_{22}N_8Cl_4Zn$: C, 41.29; H, 3.78; N, 19.27. Found: C, 41.20; H, 3.70; N, 19.17%; UV–Vis (methanol), $\lambda_{max}(\varepsilon \times 10^{-4}$, mol^{-1} cm^{-1}): 390(3.30), 280(6.89). $[HaaiHMe^{+}]_2[ZnCl_4^{2-}]$ (**9a**): *Anal.* Calc. for $C_{20}H_{22}N_8Cl_4Zn$: C, 41.29; H, 3.78; N, 19.27. Found: C, 41.35; H, 3.67; N, 19.30%; UV–Vis (methanol), $\lambda_{max}(\varepsilon \times 10^{-4}$, mol^{-1} cm^{-1}): 385 (3.56), 278 (7.68). $[MeaaiHMe^{+}]_2[ZnCl_4^{2-}]$ (**9b**): *Anal.* Calc. for $C_{22}H_{26}N_8Cl_4Zn$: C, 43.33; H, 4.27; N, 18.38. Found: C, 43.21; H, 4.20; N, 18.30%; UV–Vis (methanol), $\lambda_{max}(\varepsilon \times 10^{-4}$, mol^{-1} cm^{-1}): 388 (1.86), 280 (5.68). $[HaaiHEt^{+}]_2[ZnCl_4^{2-}]$ (**10a**): *Anal.* Calc. for $C_{22}H_{26}N_8Cl_4Zn$: C, 43.33; H, 4.27; N, 18.38. Found: C, 43.22; H, 4.33; N, 18.30%; UV–Vis (methanol), $\lambda_{max}(\varepsilon \times 10^{-4}$, mol^{-1} cm^{-1}): 390 (2.05), 280 (7.68). $[MeaaiHEt^{+}]_2[ZnCl_4^{2-}]$ (**10b**): *Anal.* Calc. for $C_{24}H_{30}N_8Cl_4Zn$: C, 45.19; H, 4.71; N, 17.57. Found: C, 45.26; H, 4.63; N, 15.67%; UV–Vis (methanol), $\lambda_{max}(\varepsilon \times 10^{-4}$, mol^{-1} cm^{-1}): 388 (3.10), 275 (7.55). $[HaaiH(CH_2Ph)^{+}]_2[ZnCl_4^{2-}]$ (**11a**): *Anal.* Calc. for $C_{32}H_{30}N_8Cl_4Zn$: C, 52.36; H, 4.09; N, 15.27. Found: C, 52.30; H, 4.03; N, 15.30%; UV–Vis (methanol), $\lambda_{max}(\varepsilon$ x 10^{-4}, mol^{-1} cm^{-1}): 400 (2.00), 305 (8.50). $[MeaaiH(CH_2Ph)^{+}]_2[ZnCl_4^{2-}]$ (**11b**): *Anal.* Calc. for $C_{34}H_{34}N_8Cl_4Zn$: C, 53.59; H, 4.47; N, 14.71. Found: C, 45.26; H, 4.63; N, 15.67%; UV–Vis (methanol), $\lambda_{max}(\varepsilon \times 10^{-4}$, mole^{-1} cm^{-1}): 395 (1.86), 280 (8.35). $[HaaiMe_2^{+}]_2[ZnCl_4^{2-}]$ (**12a**): *Anal.* Calc. for $C_{22}H_{26}N_8Cl_4Zn$: C, 43.32; H, 4.27; N, 18.38. Found: C, 43.30; H, 4.37; N, 18.24%; UV–Vis (methanol), $\lambda_{max}(\varepsilon \times 10^{-4}$, mol^{-1} cm^{-1}): 395 (2.25), 290 (7.78). $[MeaaiMe_2^{+}]_2[ZnCl_4^{2-}]$ (**12b**): *Anal.* Calc. for $C_{24}H_{30}N_8Cl_4Zn$: C, 45.18; H, 4.71; N, 17.57. Found: C, 45.22; H, 4.67; N, 17.50%; UV–Vis (methanol), $\lambda_{max}(\varepsilon \times 10^{-4}$, mol^{-1} cm^{-1}): 397 (1.89); 280 (7.68). $[HaaiEt_2^{+}]_2[ZnCl_4^{2-}]$ (**13a**): *Anal.*Calc. for $C_{26}H_{34}N_8Cl_4Zn$: C, 46.90; H, 5.11; N, 16.83. Found: C, 46.95; H, 5.07; N, 16.74%; UV–Vis (methanol), $\lambda_{max}(\varepsilon \times 10^{-4}$, mol^{-1} cm^{-1}): 400 (2.02), 295 (7.68). $[MeaaiEt_2^{+}]_2[ZnCl_4^{2-}]$ (**13b**): *Anal.*Calc. for $C_{28}H_{38}N_8Cl_4Zn$: C, 48.46; H, 5.48; N, 16.15. Found: C, 48.38; H, 5.39; N, 16.24%; UV–Vis (methanol), $\lambda_{max}(\varepsilon \times 10^{-4}$, mol^{-1} cm^{-1}): 397 (1.89), 280 (8.00). $[Haai(CH_2Ph)_2[ZnCl_4^{2-}]$ (**14a**): *Anal.* Calc. for $C_{46}H_{42}N_8Cl_4Zn$: C, 60.43; H, 4.60; N, 12.26. Found: C, 60.45; H, 4.67; N, 12.37%; UV–Vis (methanol), $\lambda_{max}(\varepsilon \times 10^{-4}$, mol^{-1} cm^{-1}): 402 (2.05), 300 (7.85). $[Meaai(CH_2Ph)_2^{+}][ZnCl_4^{2-}]$ (**14b**): *Anal.* Calc. for $C_{48}H_{46}N_8Cl_4Zn$: C, 61.19; H, 4.89; N, 11.90. Found: C, 61.25; H, 4.94; N, 12.00%; UV–Vis (methanol), $\lambda_{max}(\varepsilon \times 10^{-4}$, mol^{-1} cm^{-1}): 408 (2.43), 290 (9.58).

2.4.2. $[HaaiH_2^{+}]_2[PtCl_6^{2-}]$ (15a)

An aqueous solution of K_2PtCl_6 (60 mg, 0.123 mmol) in dilute HCl (1:1, v/v) (5 ml) was added in dropwise to methanolic solution (10 ml) of HaaiH (45 mg, 0.26 mmol). Orange-red solution was allowed to evaporate slowly for a week at 150 °C. Crystals were deposited on the wall of beakers and collected by filtration and dried over $CaCl_2$ in desiccator. Yield: 46 mg (53%). All other compounds were prepared by identical procedure in the yield of 50–70%.

All other compounds were prepared by identical procedure in the yield of 50–70%. Microanalytical data are: $[HaaiH_2^{+}]_2[PtCl_6^{2-}]$ (**15a**): *Anal.* Calc. for $C_{18}H_{18}N_8Cl_6Pt$: C, 28.64; H, 2.39; N, 14.85. Found: C, 28.51; H, 2.33; N, 14.94%; UV–Vis (methanol), $\lambda_{max}(\varepsilon \times 10^{-4}$, mole^{-1} cm^{-1}): 410 (1.68), 305 (7.85). $[MeaaiH_2^{+}]_2[PtCl_6^{2-}]$ (15b): *Anal.* Calc. for $C_{20}H_{22}N_8Cl_6Pt$: C, 25.12; H, 2.30; N, 11.72. Found: C, 25.00; H, 2.33; N, 11.90%; UV–Vis (methanol), $\lambda_{max}(\varepsilon \times 10^{-4}$, mole^{-1} cm^{-1}): 408 (2.00), 305 (7.89). $[HaaiHMe^{+}]_2[PtCl_6^{2-}]$ (**16a**): *Anal.* Calc. for $C_{20}H_{22}N_8Cl_6Pt$: C, 30.69; H, 2.81; N, 14.32. Found: C, 30.61; H, 2.75; N, 14.25; UV–Vis (methanol), $\lambda_{max}(\varepsilon \times 10^{-4}$, mol^{-1} cm^{-1}): 400 (1.90), 295 (7.55). $[MeaaiHMe^{+}]_{2p}[PtCl_6^{2-}]$ (1**6b**): *Anal.* Calc. for $C_{22}H_{26}N_8Cl_6Pt$: C, 32.59; H, 3.21; N, 13.83Found: C, 32.64; H, 3.27; N, 13.75; UV–Vis (methanol), $\lambda_{max}(\varepsilon \times 10^{-4}$, mol^{-1} cm^{-1}): 405 (2.05), 305 (8.00). $[HaaiHEt^{+}]_2[PtCl_6^{2-}]$ (**17a**): *Anal.* Calc. for $C_{22}H_{26}N_8Cl_6Pt$: C, 32.59; H, 3.21; N, 13.83. Found: C, 32.50; H, 3.25; N, 13.9; UV–Vis (methanol), λmax($\varepsilon \times 10^{-4}$, mol^{-1} cm^{-1}): 400 (2.05), 305 (9.06). $[MeaaiHEt^{+}]_2[PtCl_6^{2-}]$ (**17b**): *Anal.* Calc. for $C_{24}H_{30}N_8Cl_6Pt$: C, 34.36; H, 3.58; N, 13.36. Found: C, 34.40; H, 3.50; N, 13.40%; UV–Vis (methanol), $\lambda_{max}(\varepsilon \times 10^{-4}$, mol^{-1} cm^{-1}): 400 (2.10); 310 (7.85). $[HaaiH(CH_2Ph)+]2[PtCl_6^{2-}]$ (**18a**): *Anal.* Calc. for $C_{32}H_{30}N_8Cl_6Pt$: C, 41.11; H, 3.21; N, 11.99. Found: C, 41.23; H, 3.15; N, 12.10%; UV–Vis (methanol), $\lambda_{max}(\varepsilon \times 10^{-4}$, mol^{-1} cm^{-1}): 405 (2.25); 300 (8.85). $[MeaaiH(CH_2Ph)+]2[PtCl_6^{2-}]$ (**18b**): *Anal.* Calc. for $C_{34}H_{34}N_8Cl_6Pt$: C, 42.40; H, 3.53; N, 11.64. Found: C, 42.34; H, 3.60; N, 11.67%; UV–Vis (methanol), $\lambda_{max}(\varepsilon \times 10^{-4}$, mol^{-1} cm^{-1}): 425 (1.85), 315(7.55). $[HaaiMe_2^{+}]2[PtCl_6^{2-}]$ (**19a**): *Anal.* Calc. for $C_{22}H_{26}N_8Cl_6Pt$: C, 32.59; H, 3.21; N, 13.83. Found: C, 32.66; H, 3.28; N, 13.92%; UV–Vis (methanol), $\lambda_{max}(\varepsilon \times 10^{-4}$, mol^{-1} cm^{-1}): 390 (2.20), 300 (8.85). $[MeaaiMe_2^{+}]2[PtCl_6^{2-}]$ (**19b**): *Anal.* Calc. for $C_{24}H_{30}N_8Cl_6Pt$: C, 34.36; H, 3.58; N, 13.36. Found: C, 34.42; H, 3.63; N, 13.32%; UV–Vis (methanol), $\lambda_{max}(\varepsilon \times 10^{-4}$, mol^{-1} cm^{-1}): 410 (2.25), 301 (7.90). $[HaaiEt_2^{+}]2[PtCl_6^{2-}]$ (**20a**): *Anal.* Calc. for $C_{22}H_{26}N_8Cl_6Pt$: C, 36.02; H, 3.93; N, 12.93. Found: C, 36.06; H, 3.88; N, 12.90; UV–Vis (methanol), λmax($\varepsilon \times 10^{-4}$, mol^{-1} cm^{-1}): 400 (1.45), 305 (8.00). $[MeaaiEt_2^{+}]2[PtCl_6^{2-}]$(**20b**): *Anal.* Calc. for $C_{28}H_{38}N_8Cl_6Pt$: C, 37.58; H, 4.21; N, 12.53 Found: C, 37.66; H, 4.28; N, 12.47%; UV–Vis (methanol), $\lambda_{max}(\varepsilon \times 10^{-4}$, mol^{-1} cm^{-1}): 405 (2.10), 305 (8.45). $[Haai(CH2Ph)2+][PtCl_6^{2-}]$ (**21a**): *Anal.* Calc. for $C_{46}H_{42}N_8Cl_6Pt$: C, 49.55; H, 3.77; N, 10.05. Found: C, 49.45; H, 3.71; N, 10.00%; UV–Vis (methanol), $\lambda_{max}(\varepsilon \times 10^{-4}$, mol^{-1}cm^{-1}): 410 (2.30), 310 (8.50). $[Meaai(CH2Ph)_2^{+}][PtCl_6^{2-}]$ (**21b**): *Anal.* Calc. for $C_{48}H_{46}N_8Cl_6Pt$: C, 50.43; H, 4.03; N, 9.81. Found: C, 50.50; H, 4.04; N, 10.00%; UV–Vis (methanol), $\lambda_{max}(\varepsilon \times 10^{-4}$, mol^{-1} cm^{-1}): 410 (2.15), 310 (7.85).

2.5. X-ray diffraction study

The crystallographic data are shown in Table 1. Single crystals of $[Haai(CH_2Ph)H^{+}](Cl^{-})\ 2H_2O$ (**4a**) and $[MeaaiH_2^{+}\cdot H_2O]_2\ [PtCl_6^{2-}]$ (**15b**) were grown by evaporation of aqueous solution where as few drops of DMF added to methanolic solution of $[HaaiMe_2\ (1,3)]^{+}_2\ [ZnCl_4]^{2-}$ (**12a**) and evaporated to isolate crystals of $[HaaiMe_2\ (1,3)]^{+}[Me_2NH_2]^{+}\ [ZnCl_4]^{2-}$. DMF undergoes hydrolysis to generate dimethylamine which upon protonation may form $Me_2NH_2^{+}$. Suitable single crystals of **4a** (0.3 × 0.3 × 0.25 mm^3), **12a** (0.2 × 0.2 × 0.1 mm^3) and **15b** (0.17 × 0.13 × 0.05 mm^3) were mounted on a Brucker CCD area detector equipped with fine focused sealed tube graphite monochromated Mo Kα (λ = 0.71073 Å) radiation. The unit cell parameters and crystal-orientation matrices were determined for these compounds by least squares refinements of all reflections. The intensity data were corrected for Lorentz and polarization effects and an empirical absorption correction were also employed using the SAINT program. All these structures were solved by direct methods and followed by successive Fourier and difference Fourier syntheses. Full matrix least squares refinements on F^2 were carried out using SHELXL-97 with anisotropic displacement parameters for all non-hydrogen atoms. Hydrogen atoms were constrained to ride on the respective carbon or nitrogen atoms with anisotropic displacement parameters equal to 1.2 times the equivalent isotropic displacement of their parent atom in all cases. Complex neutral atom scattering factors were used throughout the experiments. All calculations were

Table 1
Summarized crystallographic data for **4a**, **12a** and **15b**.

	$[HaaiBzH^+](Cl^-).\ 2H_2O$ (**4a**)	$[HaaiMe_2\ (1,3)]^+\ [Me_2NH_2]^+\ [ZnCl_4]^{2-}$ (**12a**)	$[MeaaiH_2^+.H_2O]_2\ [PtCl_6]^{2-}$ (**13b**)
Empirical formula	$C_{16}H_{19}ClN_4O_2$	$C_{13}H_{21}Cl_4N_5Zn$	$C_{20}H_{26}Cl_8N_8O_2Pt$
Formula weight	334.80	454.52	818.28
T (K)	295(2)	294(2)	298(2)
Crystal system	orthorhombic	monoclinic	triclinic
Space group	$P2_12_12_1$	$P2_1/c$	$P\bar{1}$
Crystal size $(mm)^3$			
a (Å)	6.2183(6)	7.4248(5)	7.7841(5)
b (Å)αβγμθ	12.4867(11)	15.5073(11)	10.4269(7)
c (Å)	22.158(2)	17.7261(12)	18.2641(12)
α (°)	90.00	90.00	88.5880(10)
β (°)	90.00	90.5130(10)	85.8470(10)
γ (°)	90.00	90.00	81.0220(10
V $(Å)^3$	1720.5(3)	2040.9(2)	1460.25(17)
Z	4	4	2
μ (Mo Kα) (mm^{-1})	0.237	1.731	5.388
θ range	$1.84 < \theta < 28.33$	1.74–28.30	1.12–28.29
hkl range	$-7 \leqslant h \leqslant 8,\ -16 \leqslant k \leqslant 16,\ -29 \leqslant l \leqslant 23$	$-9 < h < 8;\ -20 < k < 15; -23 < l < 23$	$-10 < h < 10;\ -13 < k < 13; -24 < l < 23$
D_{calc} $(mg\ m^{-3})$	1.293	1.479	1.861
Refine parameters	704	208	350
Total reflections	11 003	12 775	14 632
Unique reflections	4 139	4 862	6 681
R_1[a] $[I > 2\sigma(I)]$	0.0424	0.0553	0.0425
wR_2[b]	0.1108	0.1112	0.1243
Goodness-of-fit (GOF) on F^2	0.895	0.892	1.002

[a] $R = \Sigma||F_o|-|F_c||/\Sigma|F_o|$.

[b] $wR_2 = [\Sigma w(F_o^2-F_c^2)^2/\Sigma w(F_o^2)^2]^{1/2}$, $w = 1/[\sigma^2\ (F_o^2) + (0.0695P)^2 + 0.0000P]$ for **4a**; $w = 1/[\sigma^2(F_0)^2 + (0.0470P)^2 + (2.7391P)]$ for **12a;** $w = 1/[\sigma^2(F_0)^2 + (0.0713P)^2 + (0.0000P)]$ for **13b** where $P = ((F_0^2 + 2F_c^2)/3$.

carried out using SHELXS 97 [19], SHELXL97 [20], ORTEP-3 [21], and PLATON 99 [22] program.

3. Results and discussion

3.1. Azoimidazolium chloride

1-Alkyl-2-(arylazo)imidazoles (RaaiR′) are gummy mass [14,15] while addition of HCl has isolated crystalline water soluble ionic (1:1 conducting) $[RaaiHR'^+]Cl^-$ (**1**–**4**) compounds (Scheme 1). 1,3-Di-alkyl-2-(arylazo)imidazolium chloride ($[RaaiR'_2{}^+]Cl^-$ (**5**–**7**) are prepared by alkylation of RaaiH with large excess of alkyl chloride. They are also crystalline and water soluble ionic compounds. Single crystal X-ray diffraction study of a representative compound, 1-benzyl-2-(phenylazo)imidazolium chloride, has confirmed the structure of the molecule.

The IR spectra of the compounds show broad, medium intense band centerd at 3420 cm^{-1} which is referred to (H_2O) and a medium intense band observed at 1620–1640 cm^{-1} which may be assigned to bending mode of water cluster [23]. Upon heating in the temperature range 90–110 °C the crystallized water was removed and IR spectra do not further show corresponding vibration even on exposure to air for 24 h. The –N═N- and –C═N- appear at 1400–1420 and 1600–1630 cm^{-1}, respectively.

The absorption spectrum of RaaiR′ and protonated form, $[RaaiR'H]^+Cl^-$ (**1**–**4**) and $[RaaiR'R'']^+Cl^-$ (**5**-**7**) in methanol solution show absorption band around 270–400 nm with a molar absorption coefficient in the order of 10^4 M^{-1} cm^{-1} and a tail extending into 500 nm. From the analogy with the absorption spectrum of azobenzene [24], it is likely that the large absorption band around 270–330 nm corresponds to π–π^* transitions, while the tail 370–400 nm corresponds to n–π^* transition. However, the π–π^* band exhibits bathochromic shifts by ~30 nm compared with azobenzene, while the n–π^* band shows little shift. As a consequence, the energy separation between the π–π^* and n–π^* transitions in arylazoimidazoles is narrower than that for azobenzene. The band is significantly influenced by substitutents at aryl and imidazolyl groups. This supports that both ground and excited states are influenced by substituents.

The 1H NMR spectra of the compounds **1**–**7** are taken in CD_3CN. The atom numbering pattern is shown in Scheme 1 and data are given in Supplementary material (Table S1). The proton signals are assigned on comparing with the spectra of RaaiR′ [14,15], spin-spin interaction and effect of substitution. Imidazole protons (4-, 5-H) appear as broad single resonance at 7.0–7.2 ppm. The broadening may be due to rapid proton exchange between two positions. The aryl protons (7-H to 11-H) are shifted to upfield side due to +I effect of 9-Me substituent in *p*-tolylazoimidazole molecules (**b**). 1-alkyl-2-(arylazo)imidazolium chloride (**1**–**4**) show proton resonance for R′: 1-Me as a sharp singlet at 4.33 ppm; 1-Et exhibits 1-(CH_2)- as quartet at *av.* 4.80 ppm (J = 9.0 Hz) and methyl (-Me) as triplet splitting pattern at *av.* 1.50 ppm (J = 10.0 Hz); 1-CH_2–(Ph) shows sharp singlet at 5.18 ppm 1,3-dialkyl-2-(arylazo)imidazolium chloride show a single resonance for R′ and R″: 1,3-Me_2 of **6** show a sharp singlet at 4.25 ppm; 1,3-Et_2 of $[RaaiEt_2{}^+](Cl^-)$ (**7**) exhibit 1-(CH_2)- as quartet at *av.* 4.85 ppm and methyl (-Me) as triplet splitting pattern at *av.* 1.5 ppm; 1-CH_2–(Ph) of **8** appears at 5.10 ppm.

3.2. Molecular structure of $[Haai(CH_2Ph)H^+](Cl^-),\ 2H_2O$ (**4a**)

The molecular structure of $[HaaiCH_2PhH^+](Cl^-),\ 2H_2O$ (**4a**) is shown in Fig. 1a and bond parameters are listed in Table 2. The azophenyl and imidazole rings are virtually coplanar as indicated by the torsion angle, C(1)–N(1)–N(2)–C(7), 178.91(17)° and the dihedral of two planes is 9.20(12)°. Maximum deviation of N(2) from mean plane formed by phenyl, azo and imidazole groups is 0.050(2) Å. Nonplanarity of benzylic phenyl group (C(11)–C(16)) with imidazole ring is due to –CH_2- group. The loss of planarity may be due to the result of 1-CH_2Ph group in the imidazole ring. The N(1)–N(2) bond length is 1.258(3) Å which is comparable to the reported data [25–27] 1.252(2) Å for 1-methyl-2-(phenylazo)imidazolium perchlorate. The N═N bond length is shorter than that of the reported distance (1.267(3) Å)

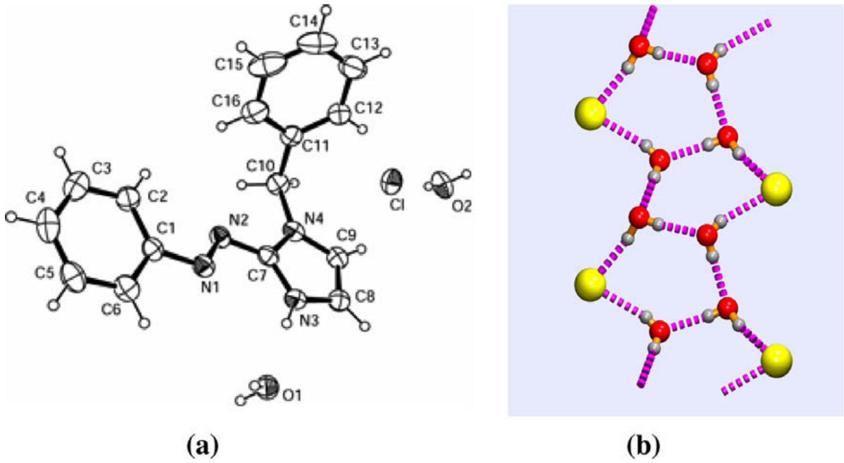

(a) (b)

Fig. 1. (a) The molecular structure of $[HaaiCH_2PhH^+]Cl^-$, $2H_2O$ with atom numbering scheme, (b) water–chloride pentameric tape constituted by $[Cl(H_2O)_4]^-$ unit.

Table 2
Selected bond length (Å) and bond angles (°) of $[HaaiCH_2PhH^+]Cl^-$, $2H_2O$ (**4a**).

Bond length (Å)		Bond angle (°)	
N(1)–N(2)	1.2574(25)	N(2)–N(1)–C(1)	115.35(18)
N(1)–C(1)	1.4156(27)	N(1)–N(2)–C(7)	110.76(17)
N(2)–C(7)	1.3964(26)	C(7)–N(3)–C(8)	108.95(17)

for 1-ethyl-2-(naphthyl-azo)imidazolium hexafluorophosphate [27]. The steric crowding and better electron donating ability of naphthyl group may be reason for the elongation. The N(azo)–C(imidazole), N(2)–C(7), 1.393(3) Å, is shorter than N(azo)–C(phenyl), N(1)–C(1), 1.418(3) Å which indicates a stronger intramolecular interaction between azo and imidazole group.

The imidazolium ion is formed by protonation of N(3) center of imidazole. Presence of Cl^- balances charge of the species. H_2O molecules are hydrogen bonded with Cl^- and constitute an aquated charged species $[Cl(H_2O)_4]^-$ (Fig. 1b). Water, the most important molecule for life, due to its hydrogen bonding ability in various cooperative modes can form water oligomers and polymers having various shapes and topology [28–56]. Reports of polymeric water association are relatively recent, only chain, tape and layer type geometries have been observed [53–56]. Water pentamer which generally has been observed to have fused tape like structure in the crystalline host [56] is the dominant constituent of liquid water at 298 K. Anomalous thermodynamic properties of liquid water has been proposed to be the result of fluctuation of number of pentamers at that temperature. Water anion associations are gaining prominence recently [57,58] due to their importance in solvation phenomena and biological ion-transport. Pentameric water tape involving Cl^- anion was evident in literarure [59,60] in which two chloride anion replaced two water molecules in the pentameric ring constituting the tape. Herein we also find a novel pentameric water chloride ring involving only one chloride anion which extends into a tape by the process of fusion of successive pentameric rings through a common edge (Fig. 1b). The anionic chain is further hydrogen bonded to arylazoimidazolium ion. Two sides of the supracycle are attached to the protonated imidazole *via* hydrogen bonding imidazole-N^+–H···$O(H_2)$. Pendant phenyl ring and 1-benzyl group undergo $\pi\cdots\pi$ interaction with neighboring partners resulting a π-sheet**.** Water-chloride tapes take position inside the rectangular channel space between two layers and develop a chloride sponge (Fig. 2). Hydrogen bonds are closer to linear geometry with D–H···A angle within 164–175°. O···O distances are 2.70 Å and 2.78 Å and O—Cl distances are 3.09 Å and 3.12 Å [O(2)–H(2A)···O(1): O(2)–H(2A), 0.78(3) Å; H(2A)···O(1), 2.01(3) Å; O(2)···O(1), 2.780(3) Å;O(2)–H(2A)···O(1), 175(3)° and symmetry: $1-x$, $1/2+y$, $1/2-z$. O(1)–H(1B)···O(2): O(1)–H(1B), 0.77(4) Å; H(1B)—O(2), 1.94(4) Å; O(1)···O(2), 2.708(3) Å; O(1)–H(1B)···O(2), 171(3)° and symmetry: $1/2-x$, $-y$,$1/2+z$; O(2)–H(2B)···Cl: O(2)–H(2B), 0.73(3) Å; H(2B)···Cl, 2.42(3) Å; O(2)—Cl, 3.122(2) Å; O(2)–H(2B)···Cl, 164(3)$_\circ$ and symmetry: *x*, *y*, *z*. O(1)–H(1A)···Cl: O(1)–H(1A), 0.88(3) Å; H(1A)···Cl, 2.22(3) Å; O(1)···Cl, 3.091(3) Å;O(1)–H(1A)···Cl, 169(3)° and symmetry: $-x$, $-1/2+y$,$1/2-z$. C(3)–H(3)···Cg(3): C(3)–H(3), 0.96(3) Å; H(3)···Cg(3), 3.09(2) Å; C(3)···Cg(3), 3.758(3) Å; C(3)–H(3)···Cg(3), 130.0(6)° and symmetry: $-1+x$, *y*, *z*]. The cyclic chloride-water pentamer is almost planar with maximum deviation for oxygen atom ranging upto 0.22 Å from the mean plane from which the Cl^- anion deviates only by 0.01 Å. The angle between successive mean planes of adjacent fused rings is 40.91° rendering the water tape a slight zigzag topography. This value is little larger than that observed in the pure water pentameric tape [56] which is 28.7°. The tape is connected to the organic π–π stacked planes on both the edges through the weak –C–H···Cl hydrogen binding. The ribbon extends along the crystallographic [1 0 0] direction through a rectangular channel space in between two π–π stacked planes (Fig. 2). The water–chloride pentamer $(H_2O)_4Cl^-$ constituting the zigzag tape (Fig. 1b) is almost planar which is self-assembled and stabilized by hydrogen bonding interaction within itself. Only a weak C–H···Cl^- bond establishes its contact with the organic layer. The ubiquity of Cl^- and water in biological systems leads us to believe that the water–chloride association of the type presented here may aid in the deeper understanding of Cl^- and proton transport in biological systems as well in the solvation phenomena of chloride salts in water.

3.3. Azoimidazolium chlorometallates

Chlorometallates of Zn(II) and Pt(IV) have been used to synthesise azoimidazolium salts in dilute HCl medium (Eqs. 1 and 2).The mixture of acidic solution (HCl) of $ZnCl_2$ or H2[$PtCl_6$] and arylazoimidazolium chloride in aqueous solution has separated orange crystalline compounds on slow evaporation in air for a week. The composition of the compounds are established by microanalytical data, molar conductance and spectroscopic (FTIR, NMR (Supplementary material (Table S1)) data. The compounds are abbreviated $[RaaiR'H^+]_2[ZnCl_4{}^{2-}]$ (**8–11**), $[RaaiR'_2{}^+]_2[ZnCl_4{}^{2-}]$(**12–14**), $[RaaiR'H^+]_2[PtCl_6{}^{2-}]$ (**15–18**) and $[RaaiR'_2{}^+]_2[PtCl_6{}^{2-}]$(**19–21**).

$$\mathrm{ZnCl_2 + 2RaaiR' \text{ or } [RaaiR'_2{}^{+}]Cl^{-} \xrightarrow{HCl/MeOH-H_2O} \underset{\mathbf{8-11}}{[RaaiR'H^{+}]_2[ZnCl_4{}^{2-}]} \text{ or } \underset{\mathbf{12-14}}{[RaaiR'_2{}^{+}]_2[ZnCl_4{}^{2-})]}} \quad (1)$$

$$\mathrm{H_2[PtCl_6] + 2RaaiR' \textit{ or } [RaaiR'_2{}^{+}]Cl^{-} \xrightarrow{HCl/MEOHH_2O} \underset{\mathbf{15-18}}{[RaaiR'H^{+}]_2[PtCl_6{}^{2-}]} \text{ or } \underset{\mathbf{19-21}}{[RaaiR'_2{}^{+}]_2[PtCl_6{}^{2-})]}} \quad (2)$$

3.4. Spectral studies

IR bands were assigned on comparing with free ligand data [14,15]. Moderately intense stretching at 1595–1600 and 1435–1445 cm^{-1} are due to ν(C=N) and ν(N=N), respectively for both types of complexes. The ionic solids, $[RaaiR'H^{+}]_2[MCl_n]^{-}$ are soluble in acetonitrile and the solution electronic spectra were recorded in the wavelength range 250–900 nm. There are two bands corresponding to ($\varepsilon \sim 10^4$ mol^{-1} dm^3 cm^{-1}) 280–310 and 375–420 nm and the bands show bathochromic shifting by 10–30 nm compared to the precursor arylazoimidazolium chloride (**1**–**7**). On comparing with free ligand spectra [61–64], and as per discussion in previous section we may conclude that these bands are due to intramolecular charge transfer transitions.

The ^1H NMR spectra of the compounds are recorded in CD_3CN. The atoms numbering pattern are shown in Scheme 1. Data (Supplementary material (Table S1)) reveal that the signals in the spectra of the compounds are shifted to downfield side relative to free ligand values and most significant downfield shifting is observed to imidazole-protons. 4- and 5-H are shifted to higher δ by 0.2–0.4 ppm relative to free ligand values. This supports the interaction of metal ions with these protons. Imidazole protons appear at 7.2–7.4 ppm as broad singlet. Aryl signals shift as usual on Me-substitution.

3.5. Structure description of chlorometallates $[HaaiMe_2(1,3)]^{+}[Me_2NH_2]^{+}[ZnCl_4]^{2-}$ (**12a**)

The crystal structure consists of a discrete tetrahedral $[ZnCl_4{}^{2-}]$, 1,3-dimethyl-2-(phenylazo)imidazolium and N,N-dimethyl ammonium ions. Fig. 3 represents an ORTEP view of the compound with the atom numbering scheme. The $[ZnCl_4{}^{2-}]$ assumes a distorted tetrahedral geometry which is measured from the magnitude of bond lengths and bond angles (Table 3). The Zn–Cl distances lie in between 2.26 to 2.29 Å. The Cl–Zn–Cl bond angles 107–113° are description of tetrahedral angular data. The structural distortion is inconsistent with the electronic configuration of Zn(II) (d10), however, it could be assessed from hydrogen bonding and noncovalent interaction present in the supramolecule (vide infra). Dimethylammonium ion in the structure may be coming from the metal assisted hydrolysis of DMF [65] in the acidified medium. $ZnCl_4{}^{2-}$constitutes a 1-D chain via hydrogen bonding with Me2$NH_2{}^{+}$.

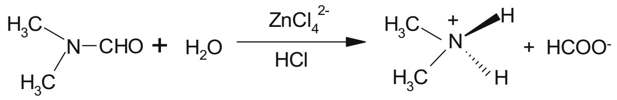

1,3-Dimethyl-2-(phenylazo)imidazolium ion is a constituent of 1-D chain by hydrogen bonding interaction with Cl of $ZnCl_4^{2-}$: N–H···Cl($ZnCl_3$) (N(5)–H(5a)···Cl(3): N(5)···Cl(3), 3.204 Å; H(5a)···Cl(3), 2.330 Å;N(5)–H(5a)···Cl(3), 163.39° Symmetry, $1-x$, $1/2+y$, 1/1 − 2 − z. N(5)– H(5b)···Cl(2): N(5)···Cl(2), 3.149 Å; H(5b)···Cl(2), 2.359 Å;N(5)–H(5b)···Cl(2), 146.45° Symmetry, $-x$,$1/2+y$, 1/1 − 2 − z) and (imidazole)C–H···Cl (C(9)–H(9)···Cl(3): C(9)–H(9)···Cl(3): C(9)···Cl(3), 3.629 Å; H(9)···Cl(3), 2.784 Å; C(9)–H(9)···Cl(3), 151.36° and symmetry, $1-x$,$1-y$,$1-z$). $HaaiMe_2(1,3)]^{+}$ forms a separate π-chain in which the basis motif is a $\pi\cdots\pi$ interacted dimmer. Both imidazole and phenyl fragments are planar. Two groups around N=N are not perfectly planar and the dihedral angle between the two least square planes is 3.4(2)°. The N=N bond length is 1.243(4) Å. The distance is slightly shorter than

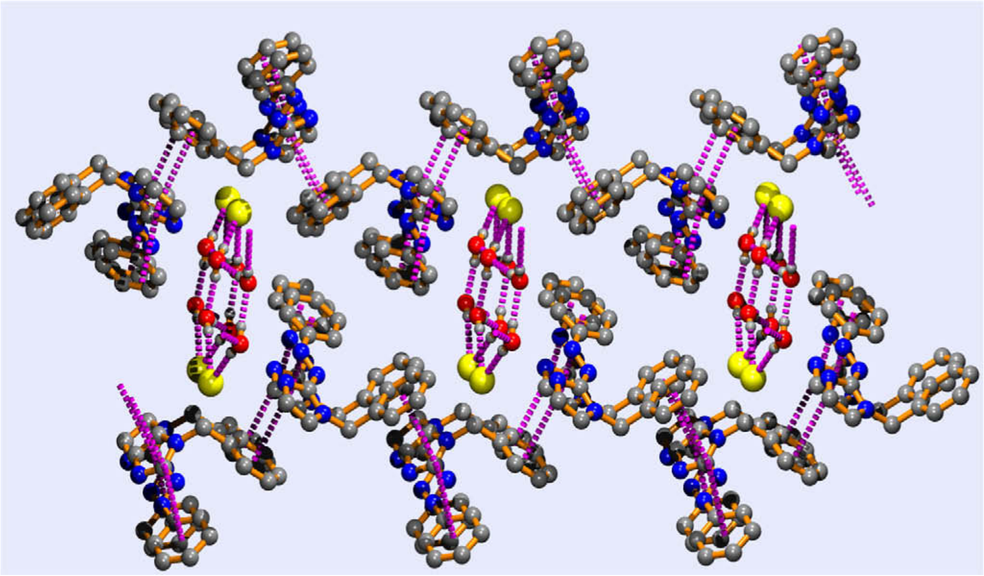

Fig. 2. Water–chloride tapes inside the rectangular channel space between two layers.

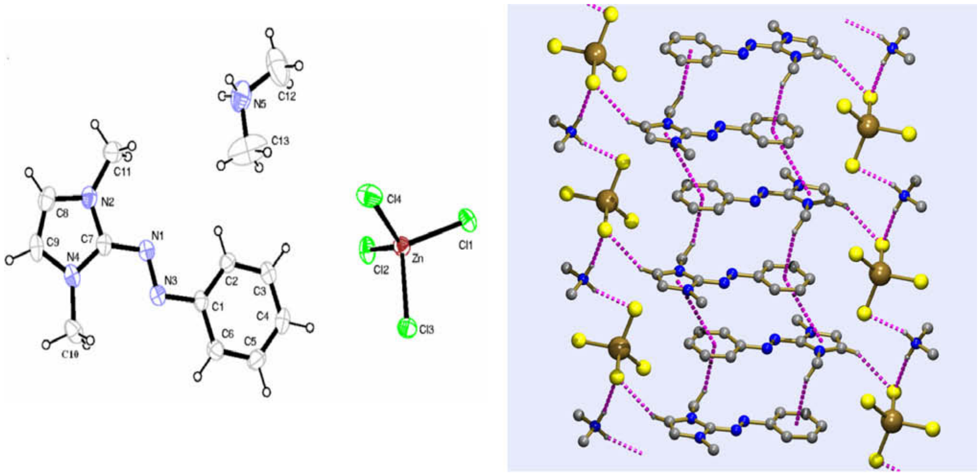

(a) (b)

Fig. 3. (a) ORTEP of [Pai-Me$_2$ (1,3)$^+$] [Me$_2$NH$_2$$^+$] [ZnCl$_4$$^{2-}$], (b) C–H···$\pi$ and π···π stacked ladder of [HaaiMe$_2$ (1,3)$^+$] [Me$_2$NH$_2$$^+$] [ZnCl$_4$$^{2-}$].

Table 3
Selected bond length (Å) and bond angles (°) of [Haai-Me$_2$ (1,3)]$^+$ [Me$_2$NH$_2$]$^+$ [ZnCl$_4$]$^{2-}$ (**12a**).

Bond length (Å)		Bond angle (°)	
Zn–Cl(1)	2.2944(10)	Cl(2)–Zn–Cl(1)	107.11(4)
Zn–Cl(2)	2.2576(11)	Cl(3)–Zn–Cl(1)	106.96(4)
Zn–Cl(3)	2.2818(10)	Cl(4)–Zn–Cl(1)	113.10(4)
Zn–Cl(4)	2.2671(11)	Cl(2)–Zn–Cl(3)	107.94(4)
C(1)–N(3)	1.418(4)	Cl(2)–Zn–Cl(4)	113.32(5)
C(7)–N(1)	1.391(4)	Cl(4)–Zn–Cl(3)	108.11(4)
N(1)–N(3)	1.243(4)	N(3)–N(1)–C(7)	113.8(3)
		N(1)–N(3)–C(1)	113.8(3)

reported data of other azoimidazole compounds (1.258 (6) Å) [7,8,17–19] and azoimidazolium ions (1.26(1) Å) [17–19]. The bonding strength between azo-N(3) and phenyl-[C(1)–N(3), 1.418(4) Å] is weaker than that of azo-N(1) and imidazole-C(7) [C(7)–N(1), 1.391(4) Å]. This suggests that the intramolecular interaction between azo and imidazole functions is stronger than that of phenyl orbital. The presence of the C–H···π interaction between C–H of imidazolyl-N-CH$_3$ of [HaaiMe$_2$ (1,3)]$^+$ and π-cloud of phenyl group (H···π, 4.191 Å, ∠C–H···π, 3.36° and symmetry: −*x*, 1 − *y*, 1 − *z*) of neighboring [HaaiMe$_2$ (1,3)]$^+$ constitutes 1-D chain (Fig. 3b). Inter-chain π···π interaction between Cgs of imidazolium ion and phenyl group of neighboring ion is Cg(Imidazolium)···Cg(phenyl): distance = 4.433 Å, α = 3.36° and symmetry: 1 − *x*, 1 − *y*,1 − *z*). These two interactions form 1-Dπ-chain. The chains are running in antiparallel fashion. This arrangement facilitates in a strong C–H···π interaction between the ring centroid (Cg) of phenyl ring and N-CH$_3$ of [HaaiMe2 (1,3)]+) [(C(10)–H(10b)···Cg(pheyl): H(10b)···Cg(phenyl), 2.816 Å; C(10)···Cg (phenyl), 3.63 Å; C(10)–H(10b)···Cg(phenyl), 143.03° and symmetry, 1 − *x*, 1 − *y*,1 - *z*) and an interaction between Cg(phenyl) and Cg(imidazole) of adjacent molecules (Cg(phenyl)···Cg(imidazole): 4.191 and 4.433 Å). Every parallel π-stacked cations are linked by two ZnCl$_4$$^{2-}$ ions on either side of the ladder through imidazolium (C(9)–H(9)···Cl(3): C(9)–H(9)···Cl(3): C(9)···Cl(3), 3.629 Å; H(9)···Cl(3), 2.784 Å;C(9)–H(9)···Cl(3), 151.36° and symmetry, 1 − *x*, 1 − *y*, 1 − *z*) which, in turn, result in a 3D supramolecular system [66].

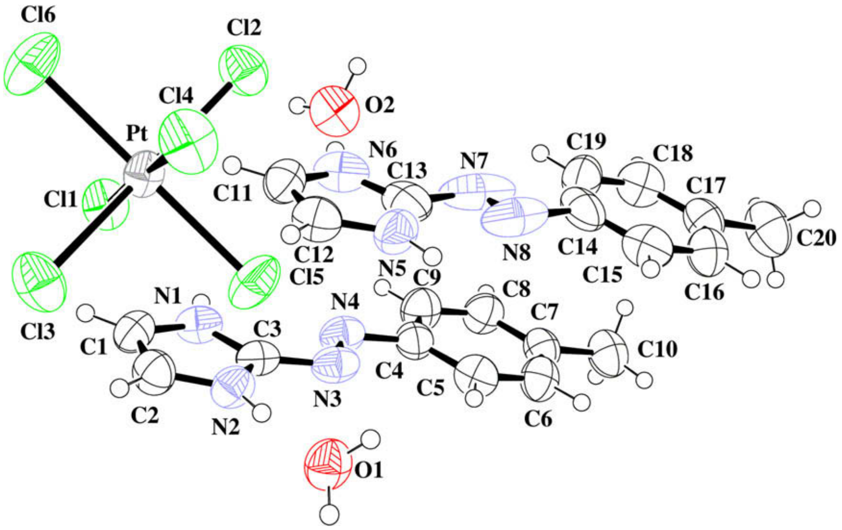

Fig. 4. Molecular view of [MeaaiH$_2$. H$_2$O$^+$]$_2$ PtCl$_6$$^{2-}$.

3.6. *[MeaaiH$_2^+$. H$_2$O]$_2$[PtCl$_6$]$^{2-}$ (**15b**)*

The crystal structure consists of a discrete octahedral $PtCl_6^{2-}$, and 2-(*p*-tolylazo)imidazolium ion. Fig. 4 represents molecular view of the compound with the atom numbering scheme. The bond lengths and bond angles are set out in Table 4. Data show slight distortion from regular octahedron. The Pt–Cl distances appear in between 2.31 to 2.33 Å. The Cl–Pt–Cl bond angles support regular geometry of the ion (cis-Cl–Pt–Cl angles exist 89–90° and trans-Cl–Pt–Cl angles are 179 to 180°). There are two 2-(p-tolylazo)imidazolium ions ($MeaaiH_2^+$) to balance charge of the anion. These two cations are in syn-configuration and two water molecules are embedded in the channel of the ions. Both imidazole and p-tolyl fragments are planar. The N=N bond lengths are N(3)–N(4), 1.214(8) and N(7)–N(8), 1.197(11) Å. The separation is 0.017 Å and is corroborated with literature data of other azoimidazole molecules [25–27]. Imidazolium ion is a good hydrogen bonding synthon. In this ionic system potential hydrogen bond acceptor is chloride (Cl in $PtCl_6$). Besides, H_2O in the molecule is a typical hydrogen bond donor and acceptor. Imidazolyl group of $MeaaiH_2^+$ is hydrogen bonded with Cl of $PtCl_6^{2-}$ and embedded H_2O (Fig. 5) (viz., N(1)–H(1)···Cl(6): N(1)–H(1), 0.86; H(1)···Cl(6), 2.380; N(1)Cl(6), 3.236(6) Å; ∠N(1)–H(1)···Cl(6), 176.00°; symmetry, 1 – *x*, 2 – *y*,1 – *z*. N(2)–H(2a)···O(1): N(2)–H(2a), 0.86; H(2a)···O(1), 1.860; N(2)···O(1), 2.714(7) Å;N(2)–H(2a)···O(1), 176.00°. N(6)–H(6)···O(2): N(6)–H(6), 0.86; H(6)···O(2), 1.850; N(6)···O(2), 2.705(9) Å; ∠N(6)–H(6)···O(2), 173.00°. N(5)–H(5a)···Cl(5): N(5)–H(5a), 0.86; H(5)···Cl(5), 2.480; N(5)···Cl(5), 3.252(6) Å; ∠N(5)–H(5a)···Cl(5), 149.00°; symmetry, 2 – *x*, 1 - *y*, 1 – *z*. O(1)–H(1)···Cl(1): O(1)–H(1), 0.85; H(1)···Cl(1), 2.67(2); O(1)···Cl(1), 3.462(6) Å; ∠O(1)–H(1)···Cl(1), 155.0°; symmetry, 1 – *x*, 2 – *y*,1 – *z*. O(1)–H(2)···Cl(4): O(1)–H(2), 0.85; H(2)···Cl(4), 2.770; O(1)—Cl(4), 3.398(6) Å; ∠O(1)–H(2)···Cl(4), 132.0°; symmetry, 2 – *x*, 1 – y,1 – *z*. O(2)–H(2B)···Cl(3): O(2)–H(2B), 0.92(6); H(2B)···Cl(3), 2.59(6); O(2)···Cl(3), 3.507(6) Å;∠O(2)–H(2B)—Cl(3), 175(10)°; symmetry, 1 – *x*, 2 – *y*, 1 – *z* O(2)–H(2C)···Cl(4): O(2)–H(2C), 0.92(7); H(2C)···Cl(4), 2.67(8); O(2)···Cl(4), 3.481(6) Å; ∠O(2)–H(2C)···Cl(4), 148(6)°; symmetry, 2-x,2-y,1-z. C(2)–H(2)···O(1): C(2)–H(2), 0.93; H(2)···O(1), 2.430; O(1)···C(2), 3.299(9) Å;∠C(2)–H(2)···O(1), 156.00°; symmetry, 1 – *x*, 1 – *y*,1 – *z*. C(12)–H(12)···Cl(5): C(12)–H(12), 0.93; H(12)···Cl(5), 2.76(2); C(12)···Cl(5), 3.658(7);∠C(12)–H(12)···Cl(5), 64.0°). Thus, two $MeaaiH_2^+$ is connected by hydrogen bonded H_2O to form 1D chain. Structure shows that each 1D chain is connected by hydrogen bonded H_2O and face-to-face imidazole···imidazole and p-tolyl···p-tolyl···π interactions (Figs. 5 and 6) (Cg1–Cg3^a:4.005(4); Cg1–Cg3^b: 3.873(4); Cg2–Cg4^a: 3.789(4); Cg2–Cg4^b:4.013(4) where Cg(1): N(1),C(1,)C(2),N(2),C(3); Cg(2): C(4), C(5), C(6), C(7), C(8), C(9); Cg(3): N(5), C(12), C(11), N(6), C(13); Cg(4): C(14), C(15), C(16), C(17), C(18), C(19) where superscript a and b refer to the motif in adjacent layers). Thus water molecule stitches two stacked ladder into a super ladder (Fig. 6). $PtCl_6^{2-}$ are positioned in the sheets of hydrogen bonded and π···π interacted layers of [MeaaiH$_2$.H$_2$O]+. The intercalated anions $PtCl_6^{2-}$ are threaded by hydrogen bonds with imidazolium N–H and H_2O [O(1)–H(1)···Cl(1): O(1)–H(1), 0.85; H(1)···Cl(1), 2.670; O(1)···Cl(1), 3.462(6) Å; ∠O(1)– H(1)—Cl(1), 155.00°; symmetry, 1-x,2-y,1-z. O(2)–H(2B)···Cl(3): O(2)–H(2B), 0.92(6); H(2B)···Cl(3), 2.59(6); O(2)···Cl(3), 3.507(6) Å; ∠O(2)–H(2B)—Cl(3), 175(10)°; symmetry, 1 – *x*, 2 – *y*, 1 – *z*. O(2)–H(2C)···Cl(4): O(2)–H(2C), 0.92(7); H(2C)···Cl(4), 2.67(8); O(2)···Cl(4), 3.481(6) Å; ∠O(2)–H(2C)···Cl(4), 148(6)°; symmetry, 2 – *x*, 2 – *y*, 1 – *z*. O(1)–H(2)···Cl(4): O(1)–H(2), 0.85; H(2)···Cl(4), 2.770; O(1)···Cl(4), 3.398(6) Å; ∠O(1)–H(2)···Cl(4), 132.00°; symmetry, 2 – *x*,1 – *y*,1 – *z*. N(5)–H(5a)···Cl(5): N(5)–H(5a), 0.86; H(5)···Cl(5), 2.480; N(5)···6 Cl(5),

Table 4
Selected bond length (Å) and bond angles (°) of [MeaaiH$_2^+$ H$_2$O]$_2$ [PtCl$_6$]$^{2-}$(**15b**).

Bond length (Å)		Bond angle (°)	
Pt–Cl(1)	2.3297(14)	Cl(2)–Pt–Cl(1)	89.54(6)
Pt–Cl(2)	2.3292(15)	Cl(4)–Pt–Cl(1)	179.18(6)
Pt–Cl(3)	2.3244(16)	Cl(5)–Pt–Cl(1)	89.43(6)
Pt–Cl(4)	2.3228(15)	Cl(6)–Pt–Cl(1)	90.47(6)
Pt–Cl(5)	2.3239(16)	Cl(3)–Pt–Cl(2)	179.28(5)
Pt–Cl(6)	2.3193(17)	Cl(5)–Pt–Cl(3)	90.25(7)
N(3)–N(4)	1.214(8)	Cl(4)–Pt–Cl(5)	89.75(7)
N(7)–N(8)	1.197(11)	Cl(6)–Pt–Cl(5)	179.81(6)
		Cl(6)–Pt–Cl(4)	90.35(7)

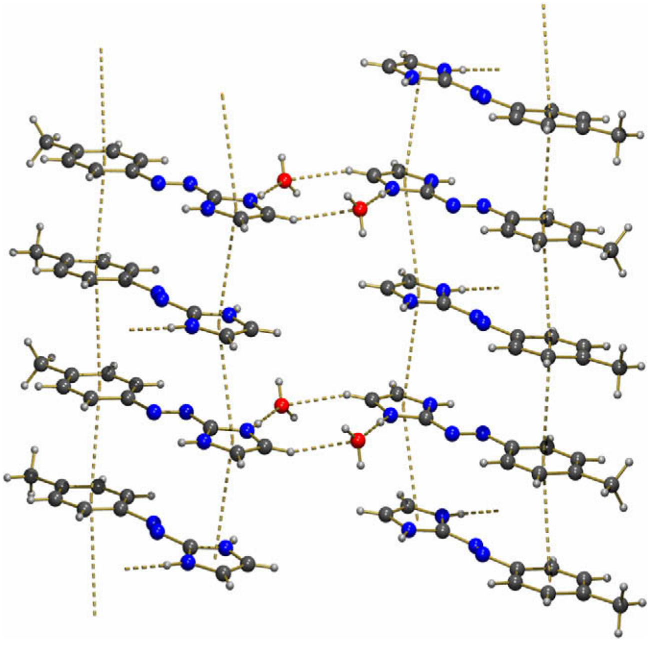

Fig. 5. Water molecule stitches two π stacked ladder into a super ladder {viewed alogn b-axis}.

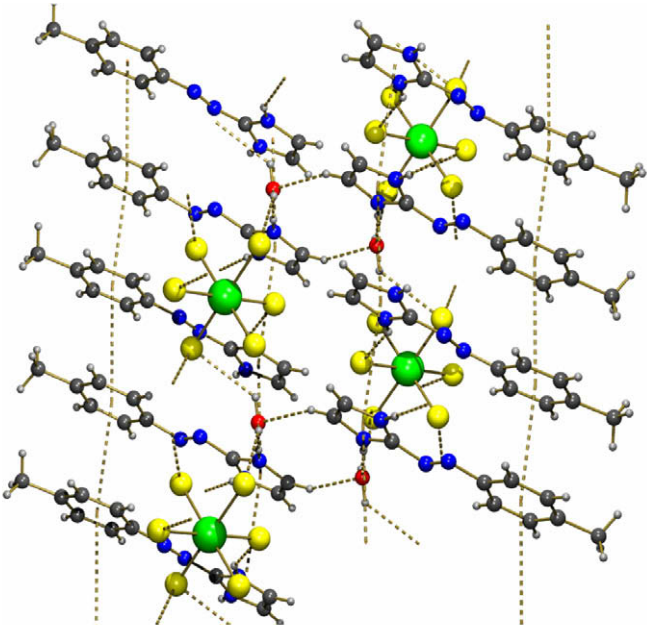

Fig. 6. Intercalated $PtCl_6^{2-}$ ⁻ in the superladder.

3.252(6) Å; ∠N(5)–H(5a)···Cl(5), 149.00°; symmetry, $2 - x, 1 - y, 1 - z$. N(1)–H(1)···Cl(6): N(1)–H(1), 0.86; H(1)···Cl(6), 2.380; N(1)···Cl(6), 3.236(6) Å; ∠N(1)–H(1)···Cl(6), 176.00°; symmetry, $1 - x, 2 - y, 1 - z$]. Imidazole C–H is also playing important role to stabilize hydrogen bonding interactions: C(12)–H(12)···Cl(5): C(12)–H(12), 0.93; H(12)···Cl(5), 2.760; C(12)···Cl(5), 3.658(7); ∠C(12)–H(12)···Cl(5), 164.00° and contribute to generate a ladder motif.

4. Conclusion

1-Alkyl-2-(arylazo)imidazoles are low melting solids or gummy mass. On acidification or alkylation they have been turned to ionic solids [RaaiR$^{/}$H^{+}](Cl^{-}) or [RaaiR$'_{2}$]$^{+(}$I^{-}). They are characterized by elemental analyses and spectroscopic studies. X-Ray structure of 1-benzyl- 2-(phenylazo)imidazolium chloride shows hydrogen bonded 1D chain. Each chain undergoes interaction with pendent (1-CH$_2$)Ph ring to constitute 2D network. Chlorometallates [MCl$_n$]$^{m-}$ also bind with dialkylated or protonated azoimidazolium ions to give stable ionic solids. Tetrahedral [ZnCl$_4$]$^{2-}$ and octahedral [PtCl$_6$]$^{2-}$ form interesting hydrogen bonded (D–H···A and C–H···π) and $\pi\cdots\pi$ interacted superstructures. Two classes of compounds are structurally characterized by single crystal X-ray diffraction studies.

Acknowledgments

Financial support from the University Grants Commission and Council of Scientific and Industrial Research, New Delhi are gratefully acknowledged.

Appendix A. Supplementary data

CCDC 246484, 637102, and 637103 contain the supplementary crystallographic data for this paper. These data can be obtained free of charge from The Cambridge Crystallographic Data Center via www.ccdc.cam.ac.uk/data_request/cif. Supplementary data associated with this article can be found, in the online version, at doi:10.1016/j.ica.2010.02.006.

References

[1] T.J. Mooibroek, C.A. Black, P. Gamez, J. Reedijk, Cryst. Growth Des. 8 (2008) 1082.
[2] A. Bianchi, K. Bowman-James, E. García-España (Eds.), Supramolecular Chemistry of Anions, Wiley, VCH, New York, 1997.
[3] Special Issue: 35 Years of Synthetic Anion Receptor Chemistry, Coord. Chem. Rev. (2003) 240.
[4] I. Ravikumar, P.S. Lakshminarayanan, E. Suresh, Pradyut. Ghosh, Inorg. Chem. 47 (2008) 7992.
[5] P.D. Beer, P.A. Gale, Angew. Chem., Int. Ed. 40 (2001) 486.
[6] J.M. Llinares, D. Powell, K. Bowman-James, Coord. Chem. Rev. 240 (2003) 57.
[7] J.L. Atwood, J.W. Steed, The Encyclopedia of Supramolecular Chemistry, Dekker, New York, 2004.
[8] K. Bowman-James, K. Acc. Chem. Res. 38 (2005) 671.
[9] K. Wichmann, B. Antonioli, T. Söhnel, M. Wenzel, K. Gloe, J.R. Price, L.F. Lindoy, A.J. Blake, E.A. Schröder, Coord. Chem. Rev. 250 (2006) 2987.
[10] Articles in Chem. Soc. Rev. 36 (2007) Issue 2.
[11] P.A. Gale, M.B. Hursthoure, T.A. Mayer, M.A. Paver, Chem. Commun. (2000) 275.
[12] P.D. Beer, Chem. Commun. (1999) 1851.
[13] V.S. Bryantsev, B.P. Hay, Org. Lett. 7 (2005) 5031.
[14] T.K. Misra, D. Das, C. Sinha, Polyhedron 16 (1997) 4163.
[15] T.K. Misra, D. Das, C. Sinha, P.K. Ghosh, C.K. Pal, Inorg. Chem. 37 (1998) 1672.
[16] U.S. Ray, B. Chand, A.K. Dasmahapatra, G. Mostafa, T.–H. Lu, C. Sinha, Inorg. Chem. Commun. 6 (2003) 634.
[17] K.K. Sarker, A.D. Jana, G. Mostafa, J.-S. Wu, T.–H. Lu, C. Sinha, Inorg. Chim. Acta 359 (2006) 4377.
[18] N.N. Greenwood, A. Earnshaw, Chemistry of Elements, Butterworth, Heinemann, London, 1997.
[19] G.M. Sheldrick, SHELXS-97 Program for the Solution of Crystal Structure, University of Gottingen, Germany, 1997.
[20] G.M. Sheldrick, SHELXL 97, Program for the Refinement of Crystal Structure, University of Gottingen, Germany, 1997.
[21] L.J. Farrugia, J. Appl. Crystallogr. 30 (1997) 565.
[22] A.L. Spek, PLATON, Molecular Geometry Program, University of Utrecht, The Netherlands, 1999.
[23] J.P. Devlin, J. Sadle, V. Buchi, J. Phys. Chem. A 105 (2001) 974.
[24] N. Nishimura, T. Sueyoshi, H. Yamanaka, E. Imai, S. Yamamoto, S. Hasegawa, Bull. Chem. Soc. Jpn. 49 (1976) 1381.
[25] P. Bhunia, B. Baruri, U.S. Ray, C. Sinha, S. Das, J. Cheng, T.–H. Lu, Transition Met. Chem. 31 (2006) 310.
[26] J. Otsuki, K. Suwa, K. Narutaki, C. Sinha, I. Yoshikawa, K. Araki, J. Phys.Chem. A 109 (2005) 8064.
[27] J. Dinda, K. Bag, C. Sinha, G. Mostafa, T.–H. Lu, Polyhedron 22 (2003) 1367.
[28] S. Manikumaei, V. Shivaiah, S.K. Das, Inorg. Chem. 41 (2002) 6953.
[29] L.R. Macgillivary, J.L. Atwood, J. Am. Chem. Soc. 199 (1997) 22592.
[30] S. Supriya, S. Manikumari, P. Raghavaiah, S.K. Das, New J. Chem. 27 (2003) 218.
[31] S. Supriya, S.K. Das, New J.Chem. 27 (2003) 1568.
[32] J.N. Moorthy, R. Natarajan, P. Venugopalan, Angew. Chem., Int. Ed. 41 (2002) 3417.
[33] S.K. Ghosh, P.K. Bharadwaj, Inorg. Chem. 42 (2003) 8250.
[34] J.L. Atwood, L.J. Barbour, T.J. Ness, C.L. Raston, P.L. Raston, J. Am. Chem. Soc. 123 (2001) 7192.
[35] R.J. Doedens, E. Yohannes, M.I. Kahn, Chem. Commun. (2002) 62.
[36] T.K. Prasad, M.V. Rajasekharan, Cryst. Growth Des. 6 (2006) 488.
[37] S.K. Ghosh, P.K. Bharadwaj, Eur. J. Inorg. Chem. 24 (2005) 4886.
[38] L.J. Barbour, G.W. Orr, J.L. Atwood, Nature 393 (1998) 671.
[39] L.J. Barbour, G.W. Orr, J.L. Atwood, Chem. Commun. (2000) 859.
[40] A. Michaelides, S. Skoulika, E.G. Bakalbassis, J. Mrozinski, Cryst. Growth Des. 3 (2003) 487.
[41] R.D. Bergougant, A.Y. Robin, K.M. Fromm, Cryst. Growth Des. 5 (2005) 1691.
[42] S.K. Ghosh, P.K. Bharadwaj, Angew. Chem., Int. Ed. 43 (2004) 3577.
[43] S. Neogi, G. Savitha, P.K. Bharadwaj, Inorg. Chem. 43 (2004) 3771.
[44] S.K. Ghosh, J. Ribas, M.S.E. Fallah, P.K. Bharadwaj, Inorg. Chem. 44 (2005) 3856.
[45] S.K. Ghosh, P.K. Bharadwaj, Inorg. Chem. 43 (2004) 6887.
[46] K. Raghuraman, K.K. Katti, L.J. Barbour, N. Pillarsetty, C.L. Barnes, K.K. Katti, J.Am. Chem. Soc. 125 (2003) 6955.
[47] P.S. Lakshminarayanan, E.I. Suresh, P. Ghosh, J. Am. Chem. Soc. 127 (2005) 13132.
[48] L.E. Cheruzel, M.S. Pometun, M.R. Cecil, M.S. Mashuta, R.J. Wittebort, R.M. Buchanan, Angew. Chem., Int. Ed. 42 (2003) 5452.
[49] S. Pal, N.B. Sankaran, A. Samanta, Angew. Chem., Int. Ed. 42 (2003) 1741.
[50] B. Sreenivasulu, J.J. Vittal, Angew. Chem., Int. Ed. 43 (2004) 5769.
[51] A. Mukiherjee, M.K. Saha, M. Nethaji, A.R. Chakravarty, Chem. Commun. (2004) 716.
[52] S. Banerjee, R. Murugavel, Cryst. Growth Des. 4 (2004) 545.
[53] M. Li, S. Chen, J. Xiang, H. He, L. Yuan, J. Sun, Cryst. Growth Des. 6 (2006) 1250.
[54] J.P. Naskar, M.G.B. Drew, A. Hulme, D.A. Tocher, D. Datta, Cryst. Eng. Comm. 7 (2005) 67.
[55] B.-Q. Ma, H.-L. Sun, S. Gao, Chem. Commun. (2004) 2220.
[56] Layer X. Luan, Y. Chu, Y. Wang, D. Li, P. Liu, Q. Shi, Cryst. Growth Des. 6 (2006) 812.
[57] D.L. Reger, R.F. Semeniuc, C. Pettinari, F. Luna-Giles, M.D. Smith, Cryst. Growth Des. 6 (2006) 1068.
[58] A.K. Ghosh, D. Ghoshal, J. Ribas, G. Mostafa, N. Ray Chaudhuri, Cryst. Growth Des. 6 (2006) 36.
[59] L. Infantes, S. Motherwell, CrystEngComm 4 (2002) 454.
[60] L. Infantes, J. Chisholm, S. Motherwell, CrystEngComm 5 (2003) 480.
[61] B.G. Chand, U.S. Ray, J. Cheng, T.-H. Lu, C. Sinha, Polyhedron 22 (2003) 1213.
[62] B.G. Chand, U.S. Ray, G. Mostafa, T.–H. Lu, C. Sinha, Polyhedron 23 (2004) 1669.
[63] B.G. Chand, U.S. Ray, G. Mostafa, T.–H. Lu, C. Sinha, J. Coord. Chem. 57 (2004) 627.
[64] B.G. Chand, U.S. Ray, J. Cheng, T.–H. Lu, C. Sinha, Inorg. Chim. Acta 358 (2005) 1927.
[65] K. Deka, M. Lasker, J.B. Baruah, Polyhedron 25 (2006) 2525.
[66] C.-K. Lam, T.C.W. Mak, Chem. Commun. (2001) 1568.